ARTICLES

Photoinduced Intramolecular Charge Transfer in Diphenylamino-Substituted Triphenylbenzene, Biphenyl, and Fluorene

Wouter Verbouwe, Lucien Viaene, Mark Van der Auweraer,* and Frans C. De Schryver*

Laboratory for Molecular Dynamics and Spectroscopy, K.U. Leuven, Celestijnenlaan 200F, 3001 Heverlee, Belgium

H. Masuhara

Faculty of Engineering, Osaka University Suita, Osaka 565, Japan

R. Pansu and J. Faure

Department of Chemistry, Ecole Normale Supérieure, 61 Av. du Président Wilson, F-94235 Cachan Cédex, France

Received: February 24, 1997; In Final Form: July 10, 1997[⊗]

The photophysical properties of a diphenyl amino-substituted triphenylbenzene, (pEFTP), biphenyl (pEFBP), and fluorene (pEFF) derivative are compared. The similarity of the photophysical properties and their solvent dependence for the triphenylbenzene and the biphenyl model compound indicate the formation of a polar excited state, localized in one branch of pEFTP. Further comparison with the fluorene model compound suggests an excited state relaxation process of the biphenyl moiety in solvents of medium and high polarity toward a more planar geometry. The depopulation of the excited state is explained in the framework of the model developed to rationalize the photophysics of substituted biphenyl.

Introduction

Although symmetric donor−acceptor substituted chromophores are expected to emit from a non polar excited state, it has been observed that photoinduced charge transfer occurs in the excited state of compounds with 2-fold (bianthryl[1,2] and biperylenyl[3]) and 3-fold (amino-substituted triphenylphosphines[4] and ruthenium(II) tris(bipyridine) complexes[5−7]) symmetry. Amino-substituted triphenylbenzene derivatives, which were developed as good hole transporting materials[8,9] emit from a highly polar excited state despite their 3-fold symmetry. The nature of the excited state of several amino-substituted triphenylbenzene derivatives has been discussed in the framework of ICT (intramolecular charge transfer) formation.[10] When a benzene ring links the electron donor and electron acceptor moiety, conjugated planar structures[11,12] as well as TICT (twisted intramolecular charge transfer) states, in which the donor moiety rotates out of the plane of the acceptor[13,14] have been proposed for the polar excited state. Due to the large fluorescence rate constants observed for most amino-substituted triphenylbenzene derivatives, the formation of a TICT state has been excluded and a planar, delocalized excited state has been suggested.[10] Furthermore, preliminary results obtained for a biphenyl model compound suggested that the excited state become localized in one branch of the amino-substituted triphenylbenzene.[15]

The excited state properties of biphenyl and substituted analogues have been a point of interest over the past decades and have been explained by Rapp and co-workers in terms of an excited state relaxation process to a planar geometry.[16] Due to the ground state steric hindrance to planarity, biphenyls are excited into twisted Franck−Condon conformations of the S_1 state. However, this state possesses a minimum for a more planar conformation. This model explained as well the presence and absence of structure in the emission and absorption spectra, respectively, as the temperature dependence of the vibrational structure of the emission spectrum of biphenyl. It can be extended to describe the analogous spectral properties in 4-alkyloxy-4′-cyanobiphenyls[17] and 4-(dimethylamino)-4′-cyanobiphenyl.[18] The relaxation occurred within the time range of 50−100 ps depending on the solvent.[17] Lahmani and co-workers used the same model as described for biphenyl to explain the large transition dipole moment of donor−acceptor biaryls derivatives substituted in the para position by cyano and *N*,*N*′-dimethylamino.[19,20] It has to be noticed that the photoinduced charge transfer process in the latter compounds occurs between the donor moiety (dimethylanilino) and the acceptor moiety (cyanophenyl). Komatsu and co-workers have studied for biphenyl the role of planarity on the rate constants for intersystem crossing.[21] It was concluded that the $T_i \leftarrow S_1$ intersystem crossing rate constant and the $S_0 \leftarrow T_1$ radiative rates are much faster in twisted biphenyls than in planar biphenyls.

In this contribution we want to focus on the radiative as well the nonradiative deactivation of the excited state of pEFTP, pEFBP, and pEFF (Figure 1). In this spectral and decay time study, the localization of the excited state in the 3-fold symmetric system is examined. In contrast to previous studies on donor substituted biphenyls,[17−19] the entire biphenyl moiety acts as acceptor.

[⊗] Abstract published in *Advance ACS Abstracts,* October 1, 1997.

S1089-5639(97)00666-X CCC: $14.00

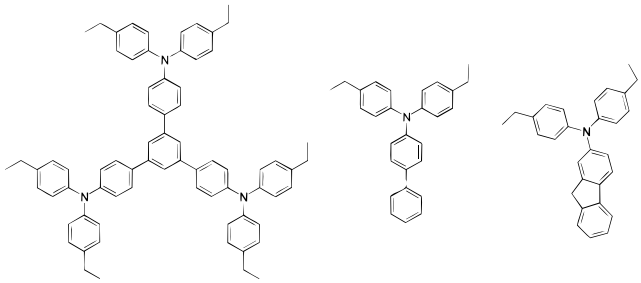

Figure 1. Structure of pEFTP, pEFBP, and pEFF.

Experimental Section

Synthesis. The preparation and purification of 5′-(4-(bis(4-ethylphenyl)-amino)phenyl)−*N*,*N*,*N*′,*N*′-tetrakis(4-ethylphenyl)−(1,1′:3′,1″-terphenyl)-4,4″-diamine (pEFTP) has been reported earlier.[22] The biphenyl (pEFBP, *N*,*N*-di(4-ethylphenyl)-(1,1′-biphenyl)-4-amine) and fluorene (pEFF, *N*,*N*-di(4-ethylphenyl)-(9*H*-fluoren)-2-amine) model compounds were synthesized in a similar way, starting from the corresponding amine. 4-Nitrobiphenyl was reduced by hydrazine monohydrate in ethanol in the presence of a Pd/C catalyst in an almost quantitative yield.[23] Without further purification, 4-aminobiphenyl was used in a second step: the substitution of the amino group to the desired biphenylamino group with 4-ethylphenyl iodide in the presence of Cu bronze, K_2CO_3, and tris(dioxa-3,6-heptyl)amine (TDA) in boiling *o*-dichlorobenzene as described previously.[22] The crude product was purified by column chromatography using silica and 1:4 dichloromethane/hexane as the eluent. NMR (400 MHz, $CDCl_3$): ^{1}H: 1.24 (6H, t, J = 7.6 Hz), 2.61 (4H, q, J = 7.6 Hz), 7.03−7.10 (10H, m), 7.27 (1H, t × t, J = 8.3, 1.4 Hz), 7.39 (2H, t × t, J = 8.3 , 1.4 Hz), 7.43 (2H, d (broad)). ^{13}C: 15.5 (CH_3, ethyl), 28.2 (CH_2, ethyl), 122.8, 124.6, 126.5, 126.6, 127.6, 128.6, 128.7 (CH, phenyl), 134.1, 138.9, 140.8, 145.4, 147.6 (C-ipso, phenyl). Mass spectrum (EI) *m*/*z* (%): 377 ($M^{+\cdot}$,100), 362 ($M^{\bullet+}$ − CH_3, 67).

The fluorene model compound was prepared in a completely similar way from 4-aminofluorene. NMR (400 MHz, $CDCl_3$): ^{1}H: 1.24 (6H, t, J = 7.6 Hz), 2.61 (4H, q, J = 7.6 Hz), 3.79 (2H, s), 7.02−7.05 (4H, m), 7.07−7.09 (5H, m), 7.20−7.24 (2H, m), 7.33 (1H, t × d, J = 7.4, 0.9 Hz), 7.47 (1H, d (broad), J = 7.4 Hz), 7.61 (1H, d, J = 8.2 Hz), 7.67 (1H, d, J = 7.4 Hz). ^{13}C: 15.5 (CH_3, ethyl), 28.2 (CH_2, ethyl), 36.8 (CH_2), 119.1, 120.1, 120.4, 122.5, 124.2, 124.8, 125.7, 126.7, 128.5 (CH, phenyl), 136.0, 138.5, 141.6, 143.0, 144.5, 145.8, 147.4 (C-ipso, phenyl). Mass spectrum (EI) *m*/*z* (%): 389 ($M^{\bullet+}$, 100), 374 ($M^{\bullet+}$ − CH_3,59).

Solvents. The solvents (isooctane, Merck; dibutyl ether, Merck; diisopropyl ether, Romil; diethyl ether, Merck; butyl acetate, Janssen Chimica; ethyl acetate, Merck; THF, Rathburn; methyl ethyl ketone, Rathburn; acetone, Romil; propionitrile, Rathburn; acetonitrile, Merck) were of spectroscopic grade and were used as received and checked for fluorescence before use.

Methods. Absorption spectra were recorded with a Perkin-Elmer Lambda 6 UV/vis spectrometer. Corrected fluorescence and excitation spectra were obtained with a SLM 8000C spectrofluorimeter in L-format. The fluorescence quantum yields were determined using quinine sulfate in 1 N H_2SO_4 as a reference (Φ_F = 0.55).[24] The fluorescence decays were obtained by the single photon timing technique.[25] For the SPT measurements an excitation wavelength of 320 nm was used and decays were measured over the whole emission range. All fluorescence decay curves were observed at magic angle (55°), contained 10 000 counts at the maximum, and were collected in 511 channels of the multichannel analyzer. The global analysis of the fluorescence decays was performed as described previously[26−28] using reference convolution. POPOP (1,4-bis-(2-(5-phenyloxazoyl))benzene) in methylcyclohexane having a decay time of 1.1 ns at room temperature was used as reference compound. For time increments bellow 10 ps/channel, a Ludox scatter solution was used instead of a reference. Fluorescence spectra and decays were obtained from samples degassed by several freeze−pump−thaw cycles. The experimental setup for the laser-induced optoacoustic spectroscopy (LIOAS) is described in detail elsewhere.[29,30] The absorbance of the sample solutions used in the LIOAS experiments was always below 0.1, and the samples were deoxygenated by bubbling argon through the solution for 15 min. Transient absorption spectra of pEFTP, from a few picoseconds up to several nanoseconds after excitation, were obtained with a pump−probe setup where a frequency tripled Nd:YAG laser and a white continuum were used for pumping and probing, respectively.[31−33] In this way, transient absorption spectra were obtained for different delays of the pump beam.

For the model compound, pEFBP, the sample was excited by the amplified and tripled pulses (35 ps) of a mode-locked picosecond Nd:YAG laser[34,35] (BMI 502 PS). The analyzing light was generated by focusing the fundamental on a tungsten electrode in a glass cell filled with xenon at a pressure of 2 bar. Both beams were focused in a nearly collinear arrangement in the middle of a cell (1 mm optical path), with an angle of 20° between both beams. After passing through a monochromator the analyzing light was detected by a streak camera (ARP, Strasbourg, France) used in single shot mode. For each data point, 20−300 traces of the analyzing pulse in the presence and absence of the excitation pulse were collected. The data were corrected for the fluorescence generated by the excitation beam and dark counts of the streak camera. The time resolution of the setup amounted 50−100 ps. This procedure was repeated every 10 or every 20 nm between 380 and 720 nm. Global analysis of transient absorption traces at different wavelengths allowed to reconstruct decay and species associated transient absorption spectra.

A frequency-tripled Nd:YAG laser pulse and a pulsed Xenon lamp as excitation and probe source, respectively, in combination whit a OMA-3 system were used to obtain transient absorption spectra 10 ns to several microseconds after excitation.[36]

Results

Steady State Spectra. The absorption maxima and shape of the absorption spectra in acetonitrile of pEFTP, pEFBP, and pEFF consist of two partially overlapping bands. The lowest absorption bands are located at 342, 324, and 334 nm for pEFTP, pEFBP, and pEFF, respectively. The second absorption band around 310 nm is similar for the three compounds. In the far-UV region a third band and the onset of a fourth band are observed around 250 and 220 nm (Figure 2). The absorption maxima and shapes of the spectra are not dependent on the solvent polarity. The conjugation of the π-system increases from pEFBP over pEFF to pEFTP which is reflected in the shift of the long-wavelength absorption band. None of the absorption spectra of the three compounds shows vibrational fine structure in any solvent.

The emission spectra in isooctane consists of a maximum at 385, 377, and 378 nm for pEFTP, pEFBP, and pEFF, respectively, and a shoulder at 400, 392, and 390 nm, respectively. In polar solvents, this vibrational structured spectrum disappears and a broad structureless band of which the maximum shifts to longer wavelengths when the solvent polarity is increased, is

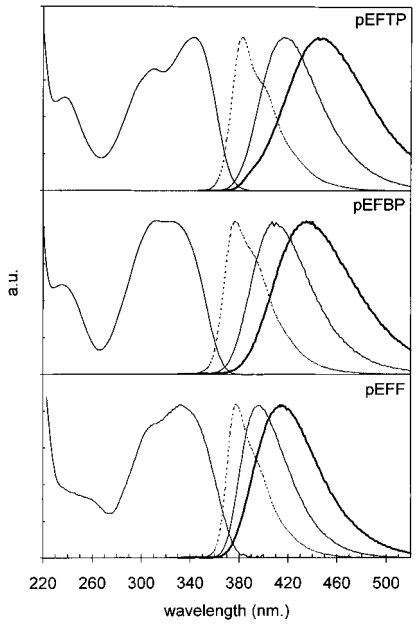

Figure 2. Absorption spectra in acetonitrile and emission spectra in isooctane (dashed), THF (full), and acetonitrile (bold) of pEFTP, pEFBP, and pEFF.

observed (Figure 2). This red shift is accompanied by a broadening of the width of the fluorescence band. The emission spectra of pEFTP and the pEFBP compound show a similar solvent dependence.

While the emission spectra of pEFF have similar features, the emission maximum is situated at shorter wavelengths and the solvatochromism is less pronounced than for pEFTP and pEFBP (Table 1). Hence the energy difference between the emission maximum of pEFBP and pEFF increases from 0.050 eV in dibutyl ether to 0.116 eV in acetonitrile.

The Lippert−Mataga relationship (eq 1a and 1b)[37,38] can be used to relate the solvent-dependent shift of the emission maximum to the change of the dipole moment upon excitation. This relationship can be simplified if the dipole moment of the ground state can be neglected. This assumption can be made as the absorption spectra of pEFTP, pEFBP, and pEFF do not depend upon the solvent. Furthermore, the dipole moment of the ground state of pEFTP is only 1.9 D.[39]

$$\bar{\nu}_F = \bar{\nu}_{F^0} - \frac{2\mu_E^2}{4\pi\epsilon_0 hca^3} F(\epsilon_r,n) \qquad (1a)$$

$$F(\epsilon_r,n) = \frac{\epsilon_r - 1}{2\epsilon_r + 1} - \frac{n^2 - 1}{2(2n^2 + 1)} \qquad (1b)$$

$\bar{\nu}_{F^0}$ and $\bar{\nu}_{F^0}$ correspond to the emission maximum (wavenumbers) in a solvent with dielectric constant ϵ_r and a refractive index $\boldsymbol{n}$, and to the emission maximum (wavenumbers) in vacuum, respectively. The constants ϵ_0, h, c, and a correspond to the permittivity of vacuum (8.85×10^{-12} C V^{-1} m^{-1}), Planck's constant (6.6×10^{-34} J s), the velocity of light in vacuum (3.0×10^8 m s^{-1}), and the radius of the solvent cavity (in m). μ_E (C m) is the dipole moment of the emitting excited state. This relationship is based on the assumptions that solvation only occurs by dipolar interactions and that the nature of the excited state does not depend on the solvent polarity. Figure 3 indicates that the experimental results do not follow this linear relationship over the whole solvent polarity range. Apparently for all the three compounds the absolute value of the slope increases in highly polar solvents like acetone and acetonitrile. A similar behavior has been observed for dimethylanilino-substituted anthracene (ADMA)[40] and has been attributed by Baumann et al.[41] to the additional shift due to the dipole−induced dipole interaction exerted by the strongly polar solute on the surrounding solvent molecules. However, to the extent that the ground state and the excited state have a similar polarizability, taking the latter effect into account is not sufficient to account for the deviations from the Lippert−Mataga plot.

The data in the polarity range from isooctane to THF could be fitted to a linear expression. Assuming a value of 7.9 and 5.5 Å for the radius of the solvent cavity in pEFTP and pEFBP or pEFF, respectively, the dipole moment of the emitting state can be calculated. The cavity radius is based on the assumption of a spherical molecule and a density of 0.8 g/cm^3. The dipole moments amount to 22, 13, and 10 D for pEFTP, pEFBP, and pEFF, respectively. To estimate the dipole moment in polar solvents, the emission maxima were for solvents ranging from methyl ethyl ketone to acetonitrile fitted to the Lippert−Mataga equation. In this way, a very high dipole moment of 40 D was obtained for pEFTP. For the other compounds, similar dipole moments were obtained for this solvent range. This suggests the contribution of other effects to the observed bathochromic shift.

The width at medium height ($\Delta\nu_{1/2}$) of the emission band can be related to the coupling of the solvation and molecular vibrations (inclusive torsions) to the electronic transition.[42]

$$\frac{(\Delta\nu_{1/2}hc)^2}{8\ln 2} = 2\lambda_0 kT + 2\lambda'_i kT + \lambda_i h\nu_i \qquad (2)$$

λ_0 corresponds to the outer-sphere solvent reorganization energy, λ'_i is the intramolecular reorganization energy associated with vibrations for which $h\nu_i < kT$, and λ_i is the intramolecular reorganization energy associated with vibrations for which $h\nu_i > kT$. The decreased flexibility of the fluorene derivative, pEFF, leads to a smaller width of the spectrum (see Table 1) compared with the biphenyl model, suggesting a difference in the equilibrium geometry of the S_1 and S_0 state. The widths of the fluorescence bands of pEFTP and pEFBP are of the same order of magnitude and stress again the similarity between the triphenylbenzene and the biphenyl compound. For a transition from an excited state with a permanent dipole moment to a ground state with a negligible dipole moment, λ_0 is given by[42]

$$\lambda_0 = \frac{\mu_E^2}{4\pi\epsilon_0 a^3} f(\epsilon_r,n) \qquad (3a)$$

$$f(\epsilon_r,n) = \frac{\epsilon_r - 1}{2\epsilon_r + 1} - \frac{n^2 - 1}{2n^2 + 1} \qquad (3b)$$

Combining eqs 1 and 3, the outer-sphere reorganization energy can be calculated for the solvent range from isooctane to THF where the Lippert−Mataga equation could be used to relate the emission maxima to the solvent polarity. The total intramolecular reorganization energy in different solvents is given by

$$\lambda'_i + \frac{\lambda_i h\nu_i}{2kT} = \frac{(\Delta\nu_{1/2}hc)^2}{16kT\ln 2} - \frac{\mu_E^2}{4\pi\epsilon_0 a^3} f(\epsilon_r,n) \qquad (4)$$

The similarity between pEFTP and pEFBP chromophores is also found for the reorganization energies (Table 1). The intramolecular reorganization energy, $\lambda_i' + \lambda_i h\nu_i/2kT$, amounts to 0.43 eV for these two compounds, while for the more planar fluorene model compound, pEFF, a value of only 0.28 eV is obtained.

TABLE 1: Photophysical Properties of pEFTP, pEFBP, and pEFF at Room Temperature[a]

		$\lambda_{max,e}$ (nm)[b]			$\Delta\nu_{1/2}$ (cm^{-1})[c]			λ_0 (eV)[d]			$\lambda'_i + \lambda_i h\nu_i/2kT$ (eV)[e]		
solv	$F(\epsilon_r,n)$	pEFTP	pEFBP	pEFF	pEFTP	pEFBP	pEFF	pEFTP	pEFBP	pEFF	pEFTP	pEFBP	pEFF
ISO	0.097	383	377	378	2555	2735	2265	3×10^{-3}	3×10^{-3}	2×10^{-3}	0.35	0.40	0.25
DBE	0.193	395	390	384	2940	3025	2465	0.06	0.06	0.03	0.41	0.44	0.26
DEE	0.256	403	397	387	3135	3245	2658	0.11	0.10	0.06	0.43	0.47	0.28
THF	0.308	417	409	397	3375	3430	2960	0.13	0.13	0.07	0.49	0.51	0.35
ACN	0.392	447	435	418	4020	4075	3626						

[a] ISO = isooctane, DBE = *n*-dibutyl ether, DEE = diethylether, THF = tetrahydrofuran, ACN = acetonitrile. [b] Emission maximum. [c] Full width at medium height. [d] Solvent reorganization energy. [e] Intramolecular reorganization energy.

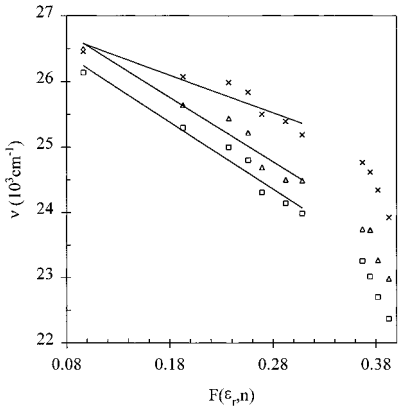

Figure 3. Emission maximum as a function of the solvent polarity for pEFTP (squares), pEFBP (triangles), and pEFF (crosses). Solvents are isooctane, *n*-dibutyl ether, diisopropyl ether, diethyl ether, butyl acetate, ethyl acetate, THF, methyl ethyl ketone, acetone, propionnitrile, and acetonitrile.

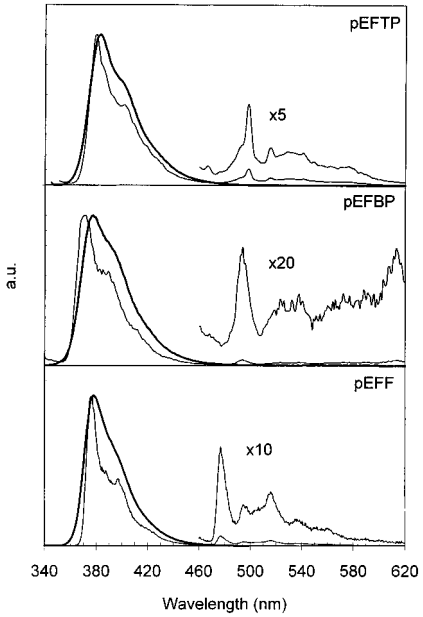

Figure 4. Emission spectra of pEFTP, pEFBP and pEFF in an isopentane glass at 77 K and in isooctane at room temperature (bold).

The emission spectra of pEFTP, pEFBP, and pEFF in isopentane glass at 77 K show two separated bands (Figure 4). Fluorescence maxima at 378, 370, and 376 nm and a shoulder at 402, 385, and 395 nm for pEFTP, pEFBP, and pEFF, respectively, are observed. Although no clear vibrational fine structure is observed, the shoulder becomes more pronounced and the bandwidth decreases at 77 K. The latter effect leads to a sharp emission band for pEFF at 376 nm. The emission maximum is shifted to higher energy at 77 K compared with the room-temperature spectrum in isooctane. For pEFBP and to a smaller extent for pEFTP,[43] the emission maximum at 77 K is shifted to shorter wavelengths compared to that at room temperature. For pEFF this shift becomes marginal.

At longer wavelengths, phosphorescence is observed with maxima for pEFTP at 498, 512, 540, and 573 nm, for pEFBP at 495, 524, 534, and 561 nm, and for pEFF at 477, 497, 516, 538, and 561 nm.

Fluorescence Decay. The fluorescence decays of the three compounds pEFTP, pEFBP, and pEFF were obtained in different solvents and at several wavelengths over the whole emission spectrum. As well using single curve analysis as global analysis linking decays at different emission wavelengths and time windows, all decays could be analyzed as a monoexponential decay. To explore the occurrence of fast processes with a decay time less than 50 ps, a time increment of 5 ps/channel is used. No indications for biexponential decays or distributions of decay rates were observed within the time resolution (20 ps) of the setup. As the fluorescence decay could be analyzed as a single-exponential decay the fluorescence rate constant, k_F, and the rate constant for radiationless decay, k_{NR}, could be obtained using the following expressions:

$$k_F = \Phi_F/\tau \tag{5a}$$

$$k_{NR} = (1/\tau) - k_F \tag{5b}$$

The similarity of the decay parameters of pEFTP and pEFBP at different solvent polarities stresses the similarity of their excited state properties (Table 2). The increase of the decay times upon increasing the polarity is mainly due to the decrease of the nonradiative decay rate in polar solvents. This increase of the decay time is to some extent due to the decrease of k_F. The latter effect is mainly due to the decrease of ν^3 upon increasing the solvent polarity. These data contrast with the important decrease of the rate constant for radiative decay and the transition dipole moment, which were observed for cyano-substituted *p*-dimethylamino biphenyls upon increasing the solvent polarity.[19] The decrease of k_{NR} is for pEFF limited to acetonitrile.

Laser-Induced Optoacoustic Spectroscopy (LIOAS). The nonradiative decay of the excited state can be factorized in the internal conversion to the ground state with a rate constant k_{IC}, and the intersystem crossing to a triplet state with a rate constant k_{ISC}. These decay parameters can be obtained by a combination of fluorescence decay analysis and laser-induced optoacoustic spectroscopy (LIOAS).[44−46] In the latter experiment, the fraction α of the absorbed laser energy, E_{abs}, that is converted into heat within the time constant of the experimental setup, E_{th}, is determined. The interpretation of the laser-induced optoacoustic experiments is based on the scheme proposed in Figure 5.

$$\alpha = E_{th}/E_{abs} \tag{6a}$$

$$\Phi_F + \Phi_{ISC} + \Phi_{IC} = 1 \tag{6c}$$

TABLE 2: Decay Parameters of the Excited Singlet State of pEFTP, pEFBP, and pEFF (for Abbreviations See Table 1)[a]

	Φ_F			τ (ns)[a]			k_F (10^7 s^{-1})[b]			k_{NR} (10^7 s^{-1})[c]			$k_F/n^2\nu^3$ (10^{-7} s^{-1} cm^3)[d]		
	pEFTP	pEFBP	pEFF	pEFTP	pEFBP	pEFF	pEFTP	pEFBP	pEFF	pEFTP	pEFBP	pEFF	pEFTP	pEFBP	pEFF
ISO	0.43	0.38	0.27	1.10	1.34	1.73	39	29	16	52	47	42	110	78	44
DBE	0.30	0.34		1.34	1.26		22	27		52	52		70	82	
DEE		0.35	0.28		1.50	1.47		23	19		43	49		80	61
THF	0.53	0.47	0.32	2.14	1.99	1.51	25	24	21	22	26	45	91	86	67
ACN	0.67	0.68	0.44	4.48	4.74	2.52	15	14	18	7	7	22	79	65	71

[a] Fluorescence decay time. [b] Rate constant of fluorescence. [c] Rate constant of nonradiative decay. [d] k_F/n^2 is proportional to the Einstein coefficient of spontaneous emission. $k_F/n^2\nu^3$ is proportional to the oscillator strength.

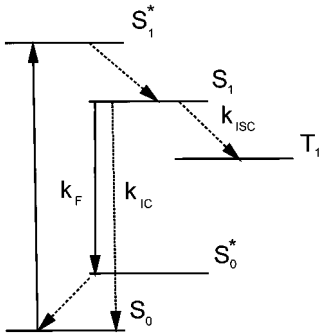

Figure 5. Scheme of the photophysical processes .

$$\alpha h\nu_{ex} = [E(S_1^*-S_1)] + \Phi_F[E(S_0^*-S_0)] + \Phi_{ISC}[E(S_1-T_1)] + \Phi_{IC}[E(S_1-S_0)] \quad (6b)$$

$E(S_1^*-S_1)$ corresponds to the energy difference between the absorption maximum and the 0−0 transition of fluorescence. $E(S_0^*-S_0)$ is the energy difference between the 0−0 transition of fluorescence and the emission maximum. $E(S_1-T_1)$ equals the difference between the 0−0 transitions of fluorescence and phosphorescence. $E(S_1-S_0)$ corresponds to the energy of the 0−0 fluorescence. $h\nu_{ex}$ is the energy of a photon at the excitation wavelength.

Due to volume changes around the polar excited triplet state, the interpretation of the LIOAS experiment could be more complicated and a more elaborated treatment of the data would be necessary. To test the validity of the approach used here, the solvent dependence of the extent of triplet formation was evaluated by comparing, for the same molecule, the $T_n \leftarrow T_1$ absorbance in solvents of different polarity. The data used here were corrected for the amount of excitation light absorbed by the sample. This implies, however, that the extinction coefficient of the $T_n \leftarrow T_1$ absorption is not solvent dependent which is probably a valid approximation as the shape of the $T_n \leftarrow T_1$ spectra does not change with the solvent polarity (cf. infra). Table 3 shows that both methods yield a parallel solvent dependence of the quantum yield of triplet formation.

k_{IC} and k_{ISC} also differ in pEFF, compared with pEFTP and pEFBP in isooctane. This suggests that for these processes the hindered rotation plays an important role. While k_F and k_{ISC} are similar for pEFTP and pEFBP, it is not so clear for k_{IC} because of the large error on these small values. For both molecules k_{ISC} decreases when the polarity of the solvent increases.

Transient Absorption. *pEFTP*. The picosecond transient absorption spectrum of pEFTP in isooctane immediately after excitation shows a maximum at 470 nm. As the decay time of this absorption signal (1.1 ns) equals the fluorescence decay time, the species absorbing at 470 nm is probably the emitting species. While the intensity of the absorption band at 470 nm decreases, a new red-shifted absorption band becomes more pronounced at longer times after excitation (Figure 6a). The latter band has a maximum around 650 nm and has also been observed 100 ns after excitation (Figure 6b). This transient absorption band has been attributed to a $T_n \leftarrow T_1$ transition.

Very similar transient absorption spectra at short and long time after excitation were observed in toluene and THF. The $S_n \leftarrow S_1$ absorption at 470 nm and the $T_n \leftarrow T_1$ at 650 nm are not dependent on the solvent polarity. Even in solvents of medium polarity like THF there is no indication for absorption by radical cation produced by photo ionization. In polar solvents like acetonitrile only ion absorption with maxima at 396 and 779 nm and a shoulder at 665 nm is observed.

pEFBP. Transient absorption traces at different wavelengths were obtained in toluene and butyl acetate. The absorption transients were fitted to the following function:

$$A(\lambda,t) = \alpha_1(\lambda)\exp(-t/\tau) + \alpha_2(\lambda) \quad (7)$$

The transient absorption traces at different wavelengths were linked, keeping the decay parameter τ constant. Good statistical parameters were obtained for the global fitting of pEFBP in toluene and butyl acetate, and a decay time (toluene 1.5 ns), similar to the fluorescence decay time, was observed. The parameters $\alpha_1(\lambda)$ and $\alpha_2(\lambda)$ allow to reconstruct decay and species associated transient absorption spectra. Therefore, $\alpha_1(\lambda)$ and $\alpha_2(\lambda)$ are proportional to following expressions:

$$\alpha_1(\lambda) \approx \sigma_{S_1\rightarrow S_n}(\lambda) - \sigma_{S_1\rightarrow S_0}(\lambda) - (1-\Phi_{ISC})\sigma_{S_0\rightarrow S_1}(\lambda) - \Phi_{ISC}\sigma_{T_1\rightarrow T_n}(\lambda)$$

$$\alpha_2(\lambda) \approx \Phi_{ISC}\,(\sigma_{T_1\rightarrow T_n}(\lambda) - \sigma_{S_0\rightarrow S_1}(\lambda))$$

$$\alpha_1(\lambda) + \alpha_2(\lambda) \approx \sigma_{S_1\rightarrow S_n}(\lambda) - \sigma_{S_1\rightarrow S_0}(\lambda) - \sigma_{S_0\rightarrow S_1}(\lambda)$$

where $\sigma_{S_1\rightarrow S_n}(\lambda)$ is the cross section for absorption to higher singlet states, $\sigma_{S_1\rightarrow S_0}(\lambda)$ cross section for induced emission, $\sigma_{S_0\rightarrow S_1}(\lambda)$ cross section for ground state absorption (depletion), $\sigma_{T_1\rightarrow T_n}(\lambda)$ cross section for triplet−triplet absorption, and Φ_{ISC} quantum yield for intersystem crossing. As for wavelength range where the spectra were recorded, ground state depletion can be neglected those expression can be simplified to

$$\alpha_1(\lambda) \approx \sigma_{S_1\rightarrow S_n}(\lambda) - \sigma_{S_1\rightarrow S_0}(\lambda) - \Phi_{ISC}\sigma_{T_1\rightarrow T_n}(\lambda)$$

$$\alpha_2(\lambda) \approx \Phi_{ISC}\sigma_{T_1\rightarrow T_n}(\lambda)$$

$$\alpha_1(\lambda) + \alpha_2(\lambda) \approx \sigma_{S_1\rightarrow S_n}(\lambda) - \sigma_{S_1\rightarrow S_0}(\lambda)$$

The decay-associated transient absorption spectrum of the singlet is given by $\alpha_1(\lambda) + \alpha_2(\lambda)(t=0)$. The induced emission gives rise to a negative absorbance and determine the transient absorption spectrum at short wavelengths. The maximum of the singlet−singlet absorption is located at 460 nm both in toluene (Figure 7a) and butyl acetate but can be shorter due to competition with induced emission.

TABLE 3: Rate Constants for the Nonradiative Deactivation of the Excited State, k_{IC} (Internal Conversion) and k_{ISC} (Intersystem Crossing), Quantum Yield of Triplet Formation, Φ_{ISC}, and $T_n \leftarrow T_1$ Absorbance Corrected for Absorbed Light ($S_1 \leftarrow S_0$)

	k_F (10^7 s^{-1})			k_{IC} (10^7 s^{-1})			k_{ISC} (10^7 s^{-1})			Φ_{ISC}			$A(T_n \leftarrow T_1)/A(S_1 \leftarrow S_0)$		
	pEFTP	pEFBP	pEFF	pEFTP	pEFBP	pEFF	pEFTP	pEFBP	pEFF	pEFTP	pEFBP	pEFF	pEFTP	pEFBP	pEFF
ISO	39	29	16	10	2	36	42	44	6	0.46	0.59	0.10	0.45	1.06	0.63
THF	25	24	21	4	3	18	18	22	37	0.38	0.45	0.49	0.21	0.89	0.88

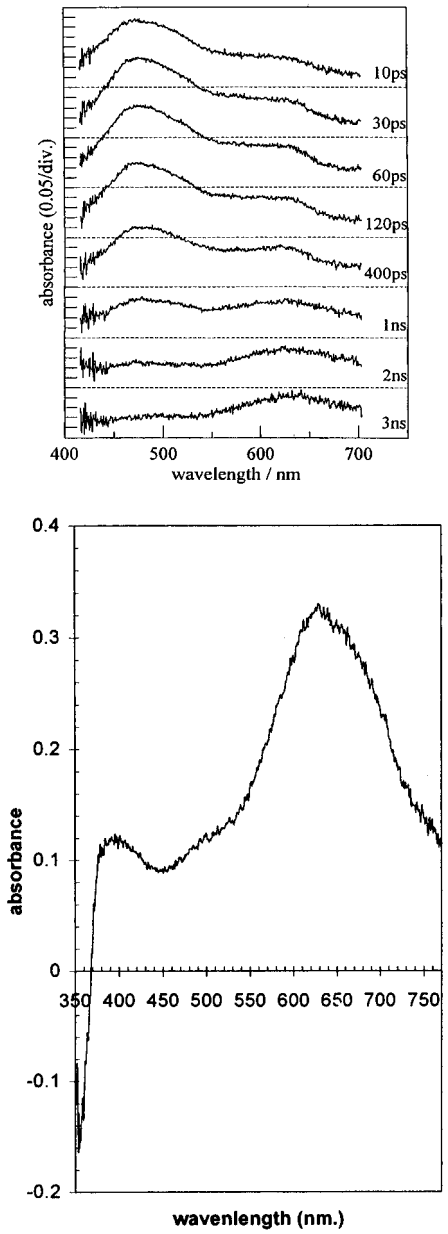

Figure 6. Transient absorption spectra of pEFTP isooctane: (a, top) picosecond transient absorption spectra from 10 ps to 3 ns after excitation, and (b, bottom) nanosecond transient absorption spectra 100 ns after excitation.

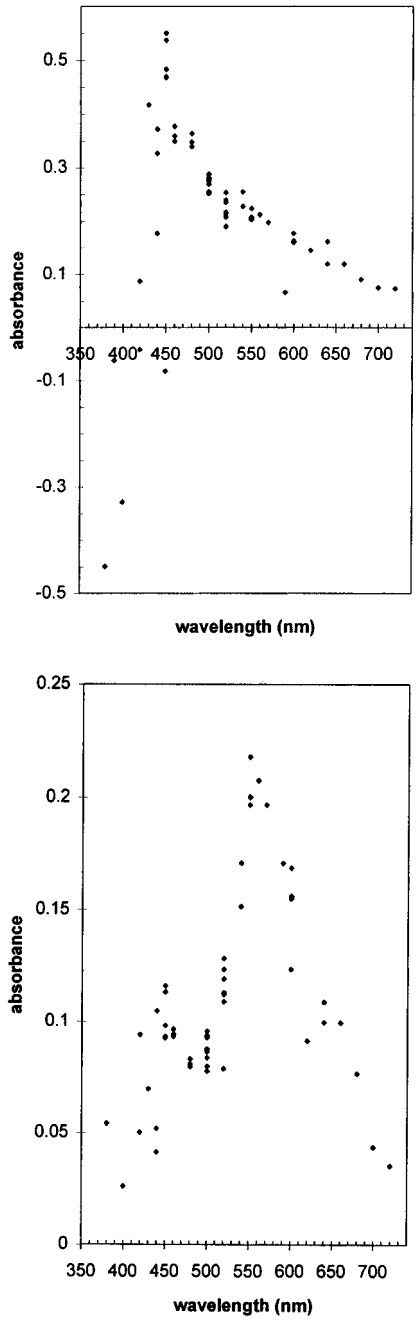

Figure 7. Decay associated transient absorption spectra of pEFBP in toluene (a, top) at short time ($\alpha_1(\lambda) + \alpha_2(\lambda)$) and (b, bottom) at long time ($\alpha_2(\lambda)$) after excitation.

The transient absorption spectra long time after excitation is given by $\alpha_2(\lambda)(t=\infty)$. The maximum of the decay associated transient absorption spectrum is situated at 550 nm in toluene and butyl acetate (Figure 7b), which is similar to the $T_n \leftarrow T_1$ absorption 100 ns after excitation where a maximum is observed at 557, 564, and 564 nm in isooctane, THF, and acetonitrile, respectively. The transient absorption spectra show even in butyl acetate or THF no absorption characteristic for radical cation of the donor moiety or the radical anion of the acceptor moiety. Those absorption maxima of those species would be situated at 712 and 630 nm for diphenylamino cation and at 380, 396, and 655 nm and at 354, 410, and 555 nm for biphenyl and triphenylbenzene anion, respectively.[47] In acetonitrile ion absorption is observed 100 ns after excitation with maxima at 380 and 750 nm and shoulder at 670 nm. This corresponds well with the nanosecond transient absorption spectrum of pEFTP in acetonitrile.

In contrast to the fluorescence spectra, where a solvatochromic shift of the emission maximum is observed, the $S_n \leftarrow S_1$ absorption is not solvent dependent.

Although the singlet transient absorption spectra of pEFTP and the model compound are very similar, this is not the case for the triplet−triplet absorption spectra, obtained using laser flash photolysis. This suggests that the triplet excited state in pEFTP is delocalized over the whole molecule.

Discussion

1. pEFTP−pEFBP. The photophysical properties of pEFTP and pEFBP are very similar. They both absorb and emit in the same wavelength region and have a similar solvent dependence. Furthermore, the singlet excited state decays with similar kinetic parameters and gives rise to similar $S_n \leftarrow S_1$ transient absorption spectra. Therefore, the polar excited state of pEFTP should be considered as localized in one branch of the molecule. This has also been concluded for the excited state of ruthenium(II) tris(bipyridine) complexes.[5] The similarity of the evolution of the emission energy of pEFTP and pEFBP in a large range of solvents polarities (Figure 3) suggests that the triphenylamino substituents in 3 and 5 position have only a limited influence on the excited state properties of pEFTP. This can be probably related to the fact that these moieties, which are expected to act as weak acceptors, are rotated out of the plane of the triphenylbenzene moiety (propeller structure).

The different dipole moments of the emitting state of pEFTP and pEFBP could be an artifact due the overestimation of the radius of the solvent cavity in the triphenylbenzene derivative. If the excitation is localized in one branch, a radius of 5.5 Å as used for pEFBP should be more appropriate than 7.9 Å for pEFTP. In this case, a smaller dipole moment of 13.0 D is found which is similar to the excited state dipole moments of pEFBP. Those dipole moments are significantly smaller than the values that would be expected for a TICT state.[10] The difference of the absorption spectra of pEFTP and pEFBP suggests that to some extent the long-wavelength absorption band is related to the formation of a delocalized excited state. Immediately after excitation, relaxation to a localized polar excited state, from where emission takes place, occurs. In this framework, the isoenergetic intramolecular energy transfer is possible in pEFTP as has been reported for related triphenylbenzene compounds[48] and ruthenium(II) tris(bipyridine) complexes.[5] Since the singlet excited state properties of pEFTP and pEFBP are similar, the charge transfer occurs between the diphenylamino moiety and the biphenyl moiety. For this reason a TICT state, where the two phenyl groups of the biphenyl moiety in pEFBP (or in pEFTP) are orthogonal, can be excluded. Furthermore, this would lead to an excited state with a very high energy because of the low electron accepting capacity of the phenyl moiety. In contrast, the electron decoupling occurs between the two aryl moieties for donor−acceptor biaryls with cyano acceptor and dimethylamino donor.[19]

The triplet excited state of pEFTP and the biphenyl model compound differ suggesting that in the triplet state a more extensive delocalization occurs.

At 77 K, a deviation of the similar spectral properties between pEFTP and pEFBP is observed. While the emission maximum of pEFBP at 77 K in isopentane glass is hypsochromically shifted compared to the emission at room temperature in isooctane, a smaller shift has been observed for pEFTP. This would suggest that for pEFTP along the coordinates involving large-amplitude vibrations, a smaller shift of the potential energy minimum occurs upon excitation.[49] The smaller shift for pEFTP can also be attributed to a combination of inhomogeneous broadening and intramolecular energy transfer to the branch with an environment that stabilized the polar excited state most effectively.

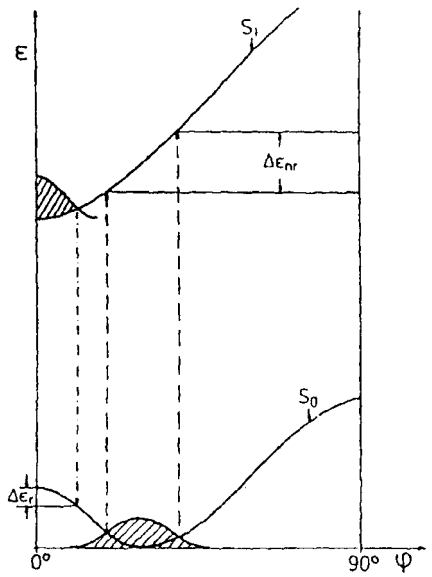

Figure 8. Twist-angle-dependent potential energy scheme for biphenyl and related compounds (according to ref 16).

2. pEFBP−pEFF. The absorption spectra of pEFBP and pEFF are similar which indicates that the initially reached excited states have the similar electronic properties. The long-wavelength absorption band of pEFF is bathochromic shifted with respect to that of pEFBP, due to the extended conjugation in the fluorene model.

The bathochromic shift of the absorption spectra is not reflected in a bathochromic shift of the fluorescence spectra. A similar result was obtained by Klock and co-workers for para-substituted cyanodimethylaminobiphenyl and an analogous fluorene derivative.[18] In spite of the better electron acceptor capacity of the fluorene moiety in pEFF, the emission occurs at slightly higher energy compared with pEFBP. Hence it is difficult to explain this difference by a different stabilization of an excited state with charge transfer character. Furthermore, the small difference of the reduction potentials, $E_{1/2} = -2.70$ and -2.65 V vs SCE in a dioxane/water (3/1) for biphenyl and fluorene, respectively,[50] suggests an identical charge distribution in the excited state. If the difference in $E_{1/2}$ would matter at all it would lead to a red-shifted emission compared with pEFBP.

Since the twisting angle between the phenyl moieties is the only important difference between pEFBP and pEFF, an explanation of this unexpected blue shift must be related to the shape of the ground state and excited state energy curves as a function of rotational angle. The intramolecular relaxation process toward a planar excited state has been reported for biphenyl and related compounds. The ground state equilibrium angle has been estimated 32°,[51] 39.5°,[52] 41.6°,[53] or 38.63° [54] in gas phase and 19°−26° [55] in solution, depending on the method used. For biphenyl, related compounds, and also for pEFBP, a lack of structure in the absorption spectrum and a structured emission band in apolar solvents is observed. This suggests a similar photophysical behavior as observed for biphenyl and related compounds. Upon excitation to an electronically delocalized and geometrically unfavorable rotated excited state, relaxation to a more planar geometry occurs. This process is too fast to be observed by the current time-resolved fluorescence technique and hence a single-exponential decay of the excited state was observed. As shown in Figure 8, fluorescence occurs to an unfavorable planar geometry in the Franck−Condon ground state, which is followed by vibrational relaxation. Both

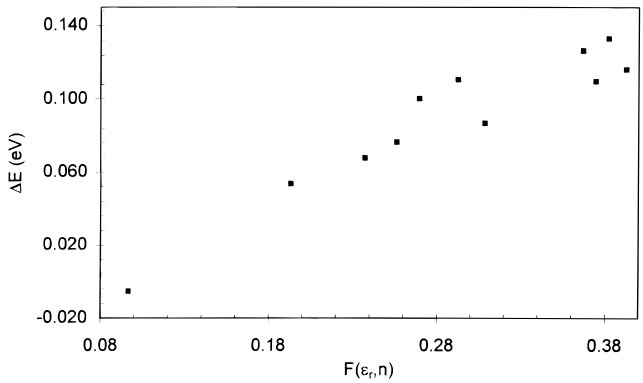

Figure 9. Energy difference between the emission maxima of pEFBP and pEFF as a function of the solvent polarity.

excited state relaxation and ground state destabilization contribute to the observed Stokes shift.

This geometric relaxation does not occur, or occurs to a considerably smaller extent, in the fluorene derivative and the emission probably takes place from the minimum of S_1 to that of the S_0 state. The reduction of the energy difference is due to this relaxation and destabilization in the Franck−Condon ground state and the latter effect does not occur in the fluorene derivative. The emission spectrum of pEFF in isopentane glass at 77 K shows no hypsochromic shift compared with the spectrum at room temperature in isooctane. This also suggests an identical geometric conformation of the S_0 and S_1 state for pEFF. In contradiction to pEFF, a hypsochromic shift from 377 to 370 nm of the emission spectra of pEFBP in isopentane at 77 K is observed. Hence the relaxation to a more planar geometry determines to a major extent the emission properties of pEFBP in apolar solvents.

Since the energy of the relaxed excited state of pEFBP and pEFF will not differ significantly, the difference of the emission maxima should be given by the difference between the minimum of the ground state and the Franck−Condon ground state. This would correspond to the rotation barrier in the ground state. For this barrier, 0.16,[56] 0.089,[54] or 0.05 eV[51] has been determined for biphenyl. The shift between pEFBP and pEFF is of the same order of magnitude as those values, keeping in mind the influence of substitution and solvation on the rotation barrier (Figure 9). In isooctane no red shift is observed because the energy difference of the relaxed singlet excited states compensates that of the Franck−Condon ground state.

Figure 9 and also Figure 3 indicate the increase of the energy difference in solvents with a higher polarity. In the framework of the proposed scheme in Figure 8, this can be explained by an increased planarity of the biphenyl part of the emitting state of pEFBP in polar solvents. This is supported by the decrease of rate constant of the intersystem crossing in the excited state of pEFBP from 4.4×10^8 s^{-1} in isooctane to 2.3×10^8 s^{-1} in THF. In the case of biphenyl, the same angular dependence of the rate constant of intersystem crossing has been found.[21] This effect can also be due to the decrease of the energy gap between the polar S_1 state and the apolar triplet state.

The picosecond transient absorption properties of pEFBP fit finally also in this scheme. Because the absorption of the emitting S_1 excited state does not change with the solvent polarity, it is difficult to assume an extensive change of the wave function in the excited state upon changing the solvent polarity. This has been proposed as possible explanation for the nonlinear Lippert−Mataga plot.[15] However, upon increasing the solvent polarity, a more extensive relaxation to a planar excited state occurs. This effect can take into account to some extent the deviations from the Lippert−Mataga plot.

The results discussed here give less information about the eventual geometric changes of the diphenylamino group with respect to the triphenylbenzene, biphenyl, or fluorene part. This is due to the fact that this group is the same for the three compounds. The smaller intramolecular reorganization energy, $\lambda_i' + \lambda_i h\nu_i/2kT$, obtained for the fluorene compound (0.28 eV in diethyl ether compared to 0.47 eV for the biphenyl compound in the same solvent) is probably mainly due to the reduction of the intramolecular relaxation of the angle between both phenyl moieties in the fluorene derivative. In contrast to the nonzero reorganization energy of 0.25 eV observed for pEFF in isooctane, the emission at 77 K in isopentane is not shifted to shorter wavelengths compared to pEFF in isooctane. Hence for pEFBP a hypsochromic shift is observed in isopentane glass which can be explained by the hindered relaxation around the two phenyl moieties in the excited state at 77 K. This suggests that no important large-amplitude vibrations of the diphenylamino part are involved in the stabilization relaxation process of the excited state in pEFF, pEFBP, and hence also pEFTP.

Acknowledgment. W.V. acknowledges the IWT for a scholarship. M.V.d.A. is an Onderzoeksdirekteur of the F.W.O.-Vlaanderen. The authors gratefully acknowledge the F.W.O., the Nationale Loterij, and the continuing support from DWTC (Belgium) through IUAP IV-11. M.V.d.A. acknowledges the E.N.S.E.T. Cachan for a stay as invited professor.

References and Notes

(1) Schneider, J.; Lippert, E. *Ber. Bunsen-Ges. Phys. Chem.* **1968**, *72*, 1155.

(2) Rettig, W. *Proc. Ind. Acad. Sci.* **1992**, *104*, 89.

(3) Dobkowski, J.; Grabowski, Z. R.; Paeplow, B.; Rettig, W.; Koch, K. H.; Müllen, K.; Lapouyade, R. *New J. Chem.* **1994**, *18*, 525.

(4) Martin, V.; Rettig, W.; Heimbach, P. *J. Photochem. Photobiol. A.: Chem.* **1991**, *61*, 65.

(5) Cooley, L. F.; Bergquist, P.; Kelley, D. F. *J. Am. Chem. Soc.* **1990**, *112*, 2612.

(6) Danielson, E.; Lumpkin, R. S.; Meyer, T. J. *J. Phys. Chem.* **1987**, *91*, 1305.

(7) Brus, L. E.; Carroll, P. J. *J. Am. Chem. Soc.* **1987**, *109*, 7613.

(8) Hartenstein, B.; Bässler, H.; Heun, S.; Borsenberger, P.; Van der Auweraer, M.; De Schryver, F. C. *Chem. Phys.* **1995**, *191*, 321.

(9) Van der Auweraer, M.; Verbeek, G.; De Schryver, F. C.; Borsenberger, P. *Chem. Phys.* **1995**, *190*, 31.

(10) Verbeek, G.; Depaemelaere, S.; Van der Auweraer, M.; De Schryver, F. C.; Vaes, A.; Terrell, D.; De Meutter, S. *Chem. Phys.* **1993**, *176*, 195.

(11) Sinha, H. K.; Yates, K. J. *J. Am. Chem. Soc.* **1991**, *113*, 6062.

(12) Carsey, T. P.; Findley, G. L.; McGlynn, S. P. *J. Am. Chem. Soc.* **1979**, *101*, 4502.

(13) Rettig, W.; Bonacic-Koutecky, V. *Chem. Phys. Lett.* **1979**, *62*, 115.

(14) Grabowski, Z. R.; Rotkiewicz, K.; Siemiarczuk, A.; Cowley, D.; Baumann, J. W. *Nouv. J. Chem.* **1979**, *3*, 443.

(15) Verbouwe, W.; Van der Auweraer, M.; De Schryver, F. C.; Pansu, R.; Faure, J. *Proceedings AIP Conference on "Fast Elementary Processes in Chemical and Biological Systems", Villeneuve d'Ascq, 1995*; Tramer, A., Ed.; Woodbury: New York, 1996; p 429.

(16) Swiatkowski, G.; Menzel, R.; Rapp, W. *J. Lumin.* **1987**, *37*, 183.

(17) Klock, A. M.; Rettig, W.; Hofkens, J.; van Damme, M.; De Schryver, F. C. *J. Photochem. Photobiol. A: Chem.* **1995**, *85*, 11.

(18) Klock, A. M.; Rettig, W. *Pol. J. Chem.* **1993**, *67*, 1375.

(19) Lahmani, F.; Breheret, E.; Zehnacker-Rentien, A.; Amatore, C.; Jutand, A. *J. Photochem. Photobiol. A.: Chem.* **1993**, *70*, 39.

(20) Lahmani, F.; Breheret, E.; Benoist d'Azy, O.; Zehnacker-Rentien, A.; Delouis, J. F. *J. Photochem. Photobiol. A.: Chem.* **1995**, *89*, 191.

(21) Fujii, T.; Suzuki, S.; Komatsu, S. *Chem. Phys. Lett.* **1978**, *57*, *2*, 175.

(22) Van der Auweraer, M.; De Schryver, F. C.; Verbeek, G.; Geelen, C.; Terrell, D.; De Meutter, S. Eur. patent EP 349034.

(23) Bavin, P. M. G. *Org. Synth. Colloid* **1973**, *5*, 30.

(24) Melhuish, W. *J. Phys. Chem.* **1961**, *65*, 229.

(25) Boens, N.; Janssens, L.; De Schryver, F. C. *Biophys. Chem.* **1989**, *33*, 77.

(26) Boens N.; Janssens L.; Ameloot M.; De Schryver, F. C. *Proceedings SPIE Conference on "Time-resolved Laser Spectroscopy in Biochemistry II", Los Angeles, 1990*; Lakowitz, R., Ed.; SPIE: Washington, DC, 1990; p 456.
(27) Ameloot, M.; Boens, N.; Andriessen, R.; Van den Bergh, V.; De Schryver, F. C. *J. Phys. Chem.* **1991**, *95*, 2041.
(28) Andriessen, R.; Boens, N.; Ameloot, M.; De Schryver, F. C. *J. Phys. Chem.* **1991**, *95*, 2048.
(29) Van Haver, Ph.; Helsen, N.; Depaemelaere, S.; Van der Auweraer, M.; De Schryver, F. C. *J. Am. Chem. Soc.* **1991**, *113*, 6849.
(30) Van Haver, Ph.; Van der Auweraer, M.; De Schryver, F. C. *J. Photochem. Photobiol. A.: Chem.* **1992**, *63*, 265.
(31) Ichakawa, M.; Fukumura, H.; Masuhara, H. *J. Phys. Chem.* **1994**, *98*, 12211.
(32) Ichakawa, M.; Fukumura, H.; Masuhara, H.; Koide, E.; Hyakutake, H. *Chem. Phys. Lett.* **1995**, *232*, 346.
(33) Fukazawa, N.; Fukumura, H.; Masuhara, H.; Prochorow, J. *Chem. Phys. Lett.* **1994**, *220*, 461.
(34) Sanquer Barrie M.; Delaire J. *New. J. Chem.* **1991**, *15*, 65.
(35) Ermolenko, L.; Delaire, J. A.; Giannotti, C. *J. Chem. Soc., Perkin Trans. 2* **1997**, in press.
(36) Van Haver, Ph.; Van der Auweaer, M.; Viaene, L.; De Schryver, F. C.; Verhoeven, J. W.; van Ramesdonk, H. J. *Chem. Phys. Lett.* **1992**, *198*, 361.
(37) Mataga, N.; Kaifu, Y.; Koizumi, M. *Bull. Chem. Soc. Jpn.* **1955**, *28*, 690.
(38) Lippert, E.; *Z. Naturforsch.* **1955**, *10a*, 541.
(39) Van der Auweraer, M.; De Schryver, F. C.; Borsenberger, P. M.; Bässler, H. *Adv. Mater.* **1994**, *6*, *3*, 199.
(40) Mataga, N.; Okada, T.; Nakashima, N.; Sakata, Y.; Misumi, S. *J. Lumin.* **1976**, *12/13*, 159.
(41) Baumann, W.; Petzke, F.; Loosen, K. D. *Z. Naturforsch. Teil A* **1979**, *34*, 1070.
(42) Brunschwig, B. S.; Ehrenson, S.; Sutin, N. *J. Phys. Chem.* **1987**, *91*, 4714.
(43) Van der Auweraer, M.; De Schryver, F. C.; Verbeek, G.; Vaes, A.; Helsen, N.; Van Haver, P.; Depaemelaere, S.; Terrell, D.; De Meutter, S. *Pure Appl. Chem.* **1993**, *65*, *8*, 1665.
(44) Van der Auweraer, M.; Viane, L.; Van Haver, Ph.; De Schryver, F. C. *J. Phys. Chem.* **1993**, *97*, *28*, 7178.
(45) Van Haver, P.; Helsen, N.; Depaemelaere, S.; Van der Auweraer, M.; De Schryver, F. C. *J. Am. Chem. Soc.* **1991**, *113*, 6849.
(46) Van Haver, P.; Van der Auweraer, M.; De Schryver, F. C. *J. Photochem. Photobiol. A: Chem.* **1992**, *63*, 256.
(47) Shida, T. *Electronic Absorption Spectra of Radical Ions*; Elsevier: Amsterdam, 1988.
(48) Schuddeboom, W.; Warman, J. M.; Van der Auweraer, M.; De Schryver, F. C.; Declerq, D. *Chem. Phys. Lett.* **1994**, *222*, 586.
(49) Van der Auweraer, M.; De Schryver, F. C.; Verbeek, G.; Vaes, A.; Helsen, N.; Van Haver, P.; Depaemelaere, S.; Terrell, D.; De Meutter, S. *Pure Appl. Chem.* **1993**, *65*, *8*, 1665.
(50) Bard, A. J.; Lund, H. *Encyclopedia of Electrochemistry of the Elements, Organic Section*; Dekker: New York, 1978; Vol. 11, p 45.
(51) Almlöf, J. *Chem. Phys.* **1974**, *6*, 135.
(52) Kobayashi, T. *Bull. Chem. Jpn.* **1983**, *56*, 3224.
(53) Almenningen, A.; Bastiansen, O. *Det. Kgl. Norsk. Vidensk. Selsk. Skrift* **1958**, *4*, 1.
(54) Haefelinger, G.; Regelmann, C. *J. Comput. Chem.* **1985**, *6(5)*, 368.
(55) Suzuki, H. *Bull. Chem. Soc. Jpn.* **1959**, *32*, 1340.
(56) McKinney, J. D.; Gottschalk, K. E.; Pedersen, L. THEOCHEM. **1983**, *13(3−4)*, 445.